60

25th U.S. Symposium on Rock Mechanics

TOPIC: Lab Fracture

SHOCK WAVE - INDUCED FRAGMENTATION OF COPPER PORPHYRIES

CATHERINE T. AIMONE, MARC A. MEYERS AND NAVID MOJTABAI

CENTER FOR EXPLOSIVES TECHNOLOGY RESEARCH
NEW MEXICO INSTITUTE OF MINING AND TECHNOLOGY
SOCORRO, NM 87801-9990

QUALIFICATIONS

The results of research presented herein are preliminary; current effort is being directed toward completing shock experiments by December 1, 1983 and finalizing all analyses by February 1, 1984.

ABSTRACT

Specimens of copper-bearing quartz monzonite were subjected to a plane shock wave simulating high compressional forces close-in to a borehole. Fragmentation was studied as a function of stress levels (between 1.3 GPa and 8.0 GPa) and pulse durations (ranging from 1μs to 6μs). Both explosive pressure and pulse duration have been shown to have a strong effect on fracturing as well as particle size distribution. Scanning electron microscopy of fragments both near the impact surface and near the specimen base were studied in order to determine the the effects of pressure and pulse duration on crack geometry and density.

INTRODUCTION

Recent interests in improving the efficiency in the comminution of ore minerals have led to studies involving the characterization of fracturing from explosive loading. Energy consumption in the mechanical crushing and grinding of ores to expose mineral constituents for benefication is less than 1% efficient (1). In 1978, electrical energy consumed to crush and grind copper ores was 18 times the energy consumed for explosive fragmentation; however, the increase in surface area per

kilowatt-hour equivalent of explosives consumed is not well understood. Conventional rock breakage using explosives in cylindrical boreholes is performed for handling ore during mining production; little attention is given during blasting to the amount of particle size reduction for processing. Fine crushing, however, occurs within a limited region surrounding the borehole.

There is considerable interest to extend this zone of finely crushed rock during explosive breakage. The mechanisms of rock breaking using multiple cylindrical charges is extremely complex. A number of experiments have been conducted in an attempt to understand the roles of stress waves, delayed gas pressures, and their interaction with reflecting free surfaces on fragmentation. As an initial step in isolating the various processes involved in fracture, a series of flyer-plate impact experiments were made to determine the effects of compressive explosive pressure and pulse duration on fragmentation for copper porphyry in the absence of reflected waves. The uniaxial loading is thought to simulate the high compression forces exerted near the borehole wall during detonation.

Rock specimens used for shock experiments were altered quartz monzonite porphyries consisting of quartz, orthoclase and abundant sericite minerals. Grain sizes range from 1mm to 5mm with 3% to 4% chalcocite as the chief ore mineral. The rock contains numerous healed fractures.

EXPERIMENTAL DESIGN AND SHOCK WAVE THEORY

Figure 1 shows the inclined plate plane-wave generator used to induce a uniaxial strain wave in a cylindrical specimen of copper porphyry quartz monzonite. The "mousetrap" assembly, as described by Benedick (2), uses Detasheet of varying thicknesses for the main explosive charge and the triangular line-wave generator. A two layered concrete containment system encased the specimen; by matching impedence (wave velocity times density) of the concrete (using barite as a heavy aggregate) with that of the quartz monzonite, the concrete served as a trap to contain outgoing shock waves; thus the reflected tensile waves were "trapped" in the concrete, allowing the momentum traps to literally tear away from the shocked specimen.

The mathematical treatment of shock waves, based on the theory for fluids, was developed by Rankine and Hugoniot (3,4). From these relations and from the Gurney equation (5) one can compute a flyer-plate velocity for a desired impact pressure, and establish a certain ratio of masses of explosive to flyer-plate. For a steady, uniaxial strain wave with a plane front, the jump relations describing changes across the shock front may be derived from the conservation laws for mass, momentum and energy. The momentum equation, relating pressure, P, density, ρ, shock velocity U_s, and for surface particle velocity U_p is

$$P - P_o = \rho U_s U_p \qquad (1)$$

To calculate the Hugoniot relationship for pressure as a function of particle velocity, a second equation relating shock velocity and particle velocity is given by:

$$U_S = C_o + S U_p \qquad (2)$$

Where C_o is the sound velocity for the material and S an empirical parameter experimentally determined. Substituting Equation (2) into (1), the relation of pressure as a function of particle velocity is given. By using the method given by Meyers and Murr (6) for polyphase materials being impacted by a 2024 aluminum flyer plate, a Hugoniot curve is drawn for quartz monzonite and a series of curves for 2024 aluminum (reverse slope), each series intersecting at the desired pressure. These curves are shown in Figure 2. From these intercepts, the free surface particle velocity for the flyer plate is given. The point at which the reversed aluminum curve intersects the particle velocity axis for a desired impact pressure corresponds to the flyer plate velocity (along the particle velocity axis).

Once the flyer plate velocity is set, the ratio of explosive to plate density (C/M) is determined for a given explosive internal energy detonating at a "grazing incidence" for the inclined plate. The ratio of explosive thicknesses to flyer plate thickness, T is given by

$$\frac{t}{T} = \frac{\rho_m}{\rho_e}\left(\frac{C}{M}\right) \qquad (3)$$

where ρm and ρe are the plate mass and explosive densities respectively. However, for a specific plate thickness, pulse duration, t_p, is given by (6)

$$t_p = \frac{2\ T}{U_s} \qquad (4)$$

The calculations above are described in greater detail by DeCarli and Meyers (7).

Sixteen experimental shots are being made for four pressure levels shown in Table 1. Particle size distributions from each shot where sufficient quantities of particles are recovery will be made; scanning electron microscopy (SEM) is being used to observe the various levels of microcracking as well as measure the density of cracking and statistical distribution of crack lengths.

At present, four shots remain to be completed for particle size distributions and SEM analysis; in addition, five shots will be performed in a second series in which shocked specimens will be set in epoxy for analysis of in-place size distribution.

TABLE 1. SUMMARY OF SHOCK-WAVE EXPERIMENTS FOR QUARTZ MONZONITE COPPER PORPHYRIES

SPECIMEN NUMBER	PRESSURE GPa	PULSE DURATION μs	PERCENTAGE OF FRAGMENTS GREATER THAN 1.27 cm	PERCENTAGE OF SPECIMEN ORIGINAL WEIGHT LOST AFTER SHOT
1.3 - 1	1.3	1*	SR	—
1.3 - 2		2*	SR	—
1.3 - 6		6*	SR	—
2.6 - 1		1*	81.0	3.1
2.6 - 2	2.6	2	74.5	7.2
2.6 - 6		6	14.6	22.3
3.2 - 2	3.2	2	65.7	9.7
5.1 - 1		1*	65.7	5.3
5.1 - 2	5.1	2	SR	—
5.1 - 6		6	--	92.0
8.0 - 1	8.0	1	77.8	53.0

*Experiments will be studied with the SEM and particle sizes analyzed; a second series of experiments will allow shocked specimens to be epoxied.

SR shots remaining.

RESULTS

Particle size distributions for comparable specimens recovered are shown in Figure 3 (a) for three pulse durations (1, 2, and 6 s) at 2.6 GPa pressure and in Figure 3(b) for three pressures (2.6, 5.1, and 8.0 GPa) at 1 μs duration. These percentages correspond to original specimen weight and not weight recovered. Therefore, material loss is apparent. Assuming material loss was represented by the finer fractions, it is readily apparent that the reduction in particle sizes in a range of

sizes greater than 5mm is substantial for increasing pulse durations at 2.6 GPa. A pulse duration increase of 6 generated a six-fold increase in fines of the 5mm size. The effects on size reduction with increasing pressure is also significant.

Cracks were observed with the SEM; selected micrographs are shown in Figures 4 through 12. Cracking is observed to be transgranular (running from grain boundary across a grain), intergranular (crossing over grain boundaries) or intragranular (a crack running partially within a single grain). Cleavage and grain boundary cracks are also prevalent.

Figures 4 through 7 were taken at the impact surface of shocked specimen 2.6-1. At high magnification, abundant cleavage fractures are shown in quartz (Figure 5). Major fractures begin, at quartz grain edges from the major grain boundary cracks between quartz and sericite shown in Figure 4, transgress to naturally occurring void and cease. Similar features are noted in Figure 8 for specimen 80-1; however, at the location central to the specimen, edge crack termination is not necessarily related to voids. Intragranular cracks in quartz not associated with grain edges are shown in Figure 12. Similar intragranular cracking is noted in sericite; however, they are associated with the orientation of the platey structure. Grain boundary cracks are common in the fine grain structures of orthoclase (Figure 9) and sericite (Figure 11).

REFERENCES

1. "Comminution and Energy Consumption", prepared by the Committee on Comminution and Energy Consumption, National Materials Advisory Board, National Academy of Sciences for the DOE, U.S.B.M., and N.S.F., May 1981, 298 pp.

2. Benedick, W.B., "Detonation Wave Shaping', in "Behavior and Utilization of Explosives in Engineering Design", eds. L. Davidson, et. al., New Mexico Station, Albuquerque, NM, 1972.

3. Rankine, W.J.M., Phil. Trans. Roy. Soc., London, 160, (1870) 270.

4. Hugoniot, J. J., L'Ecole Polytechnique 58 (1889) 3.

5. Gurney, R. W., "The Initial Velocities of Fragments from Bombs, Shells, and Grenades", Rep. 405, BRL, Aberdeen Proving Grounds, September 1943.

6. Meyers, M. A., and Murr, L. E., eds., "Shock Waves and High-Strain-Rate phenomena in Metals", Plenum Press, New York, 1981.

7. DeCarli, P. S. and Meyers, M. A., source cited in ref. 6, p. 34.

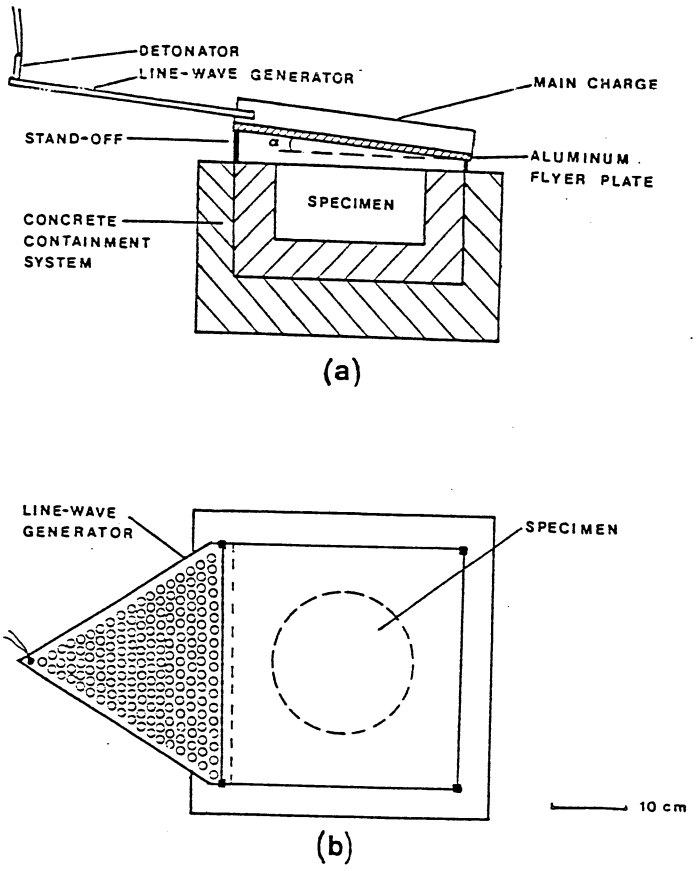

Figure 1. Plane-wave generator; (a) side view and (b) top view.

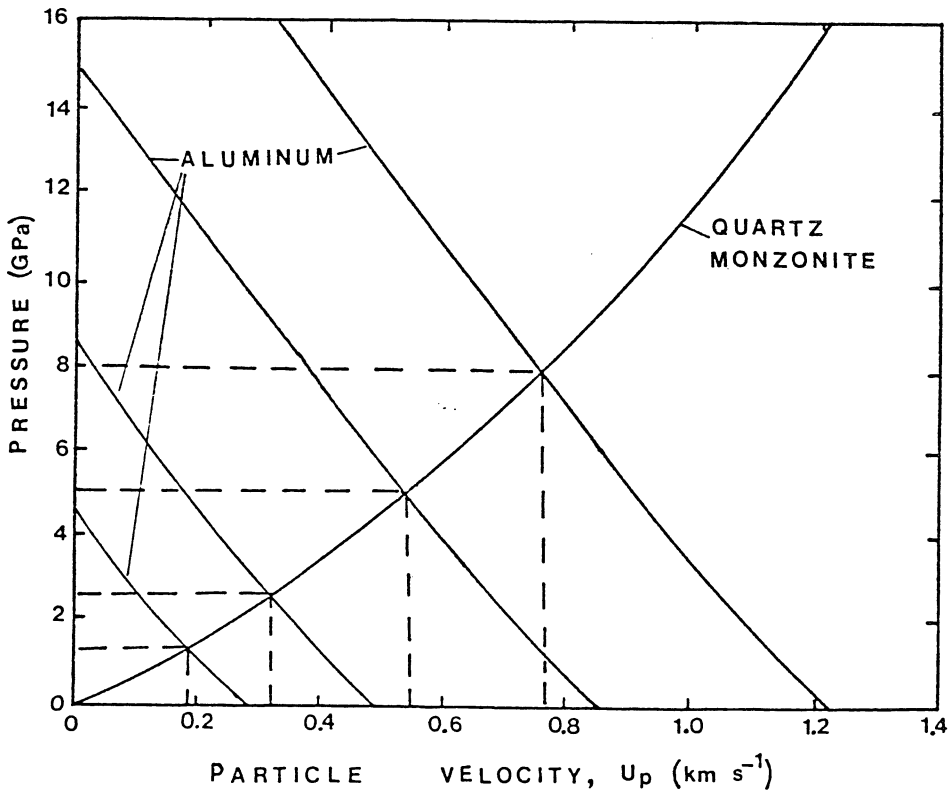

Figure 2. Shock Hugoniots (pressure versus particle velocity) for quartz monzonite and aluminum (reversed).

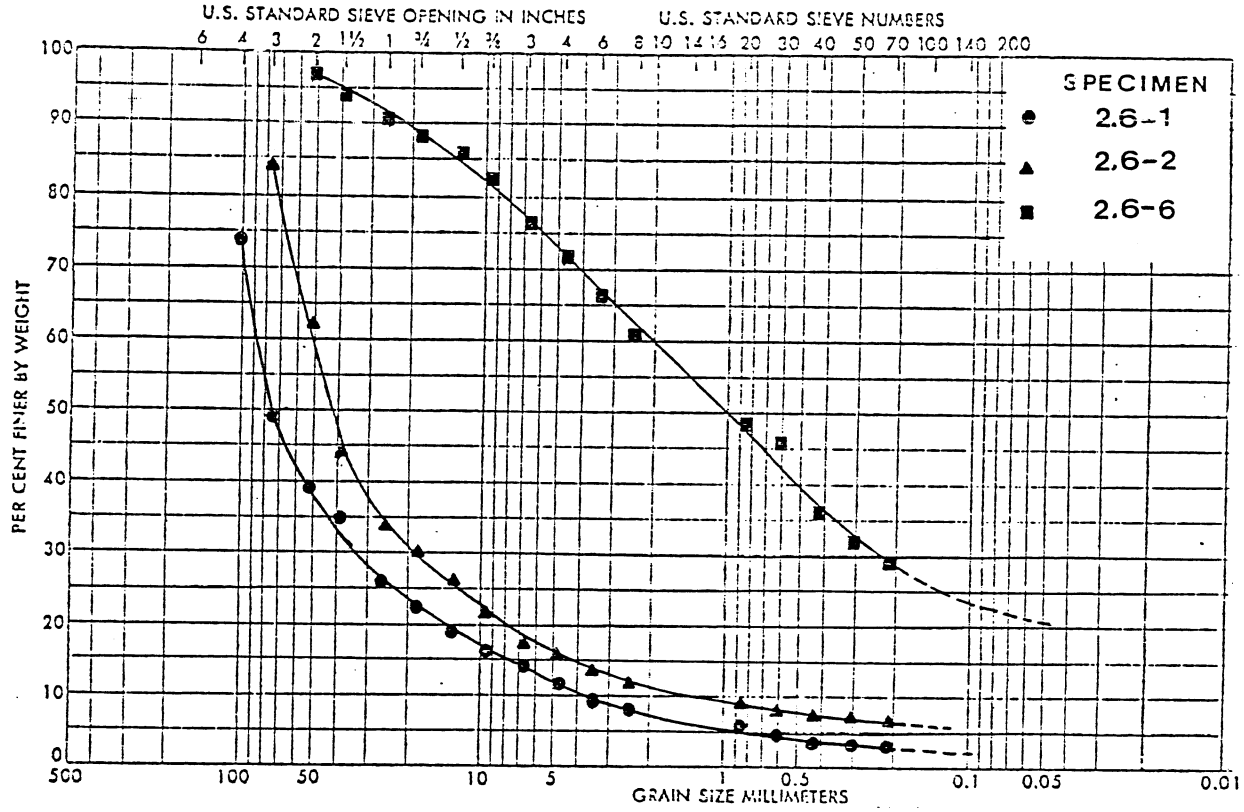

(a)

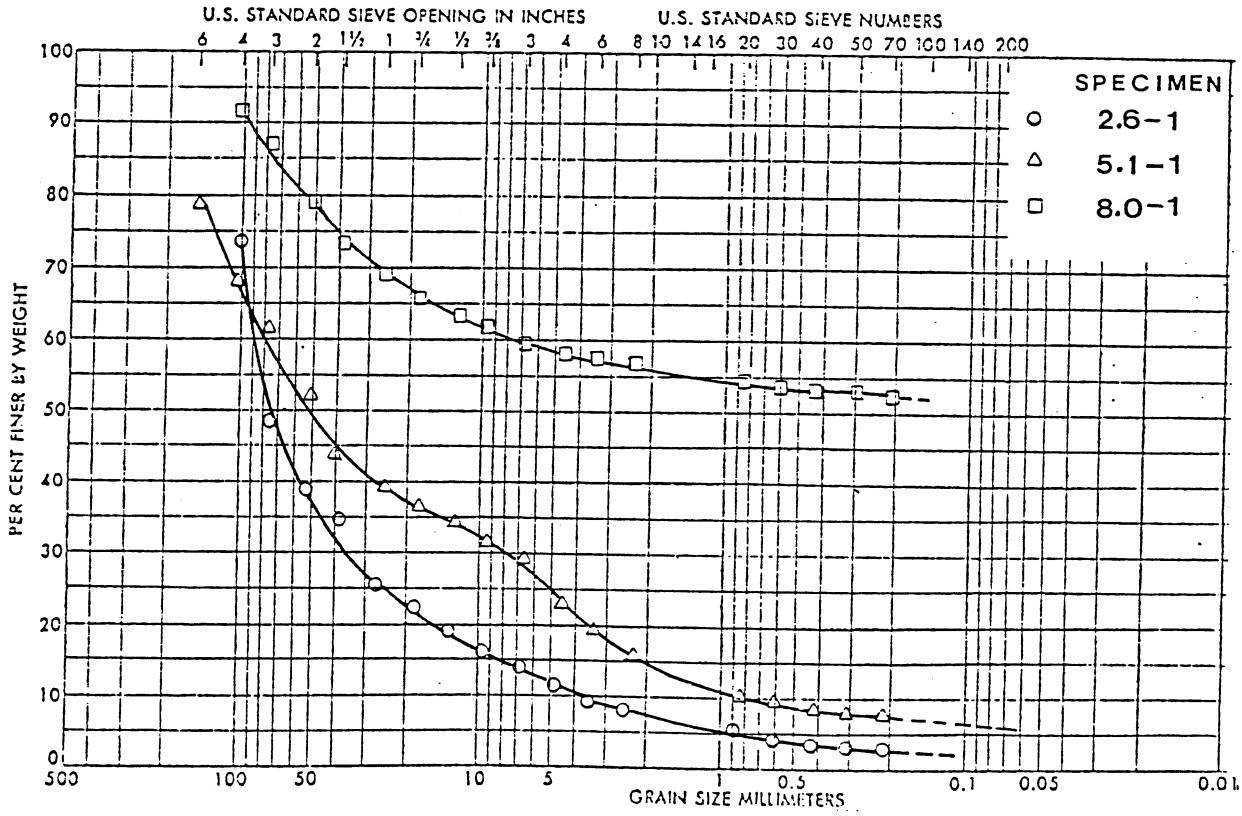

(b)

Figure 3. Cummulative Distribution of Fragments Recovered (a) For Three Pulse Durations at 2.6 GPa Pressure and (b) For a Pulse Duration of 1 us for Three Pressure Levels.

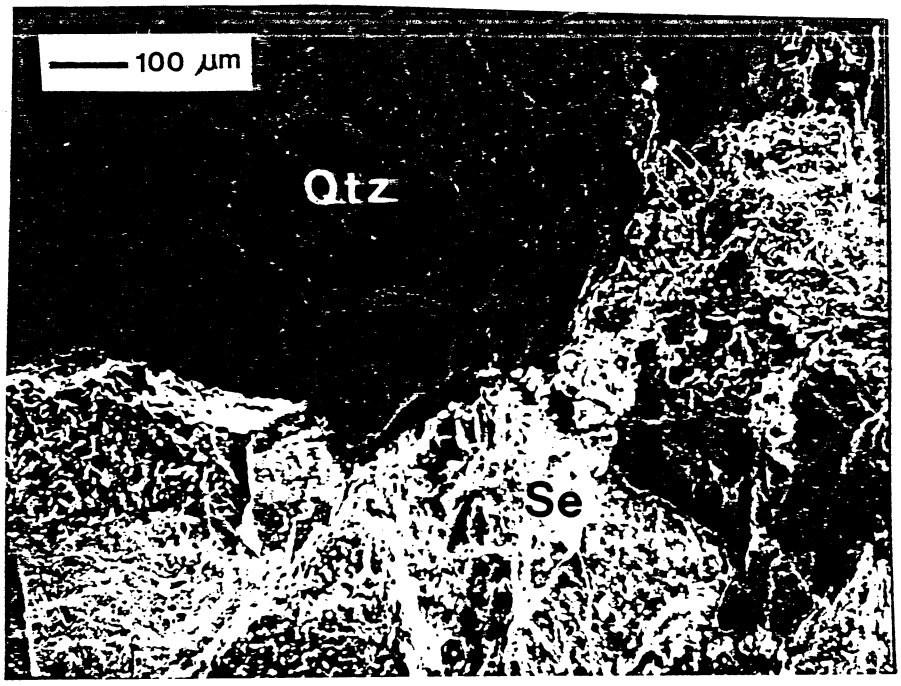

Figure 4. Scanning electron micrograph (SEM) of quartz (Qtz) and sericite (Se) in shocked specimen 2.6-1 taken near the impact surface.

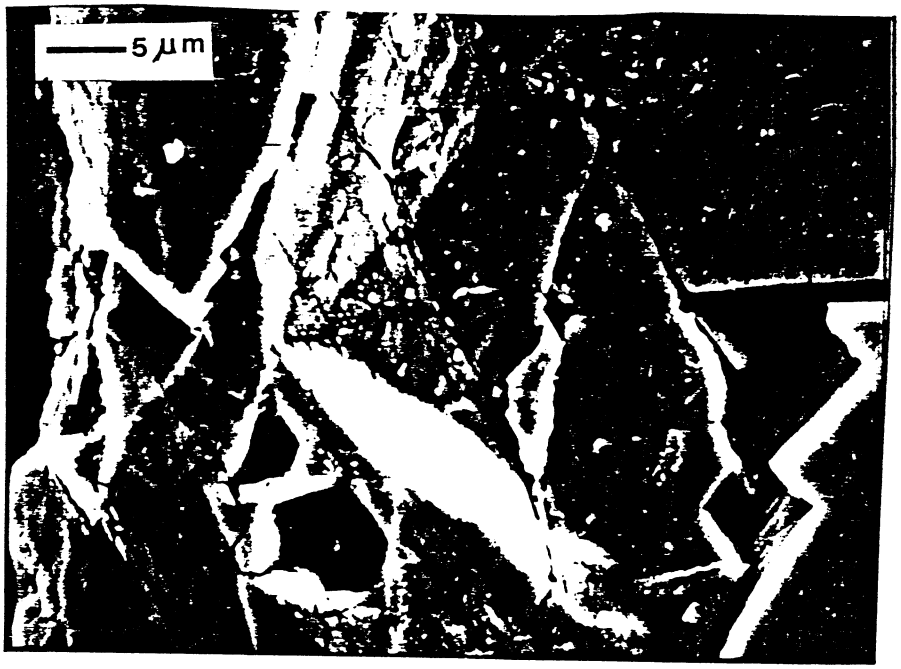

Figure 5. Abundant cleavage fractures shown for quartz region of Figure 4.

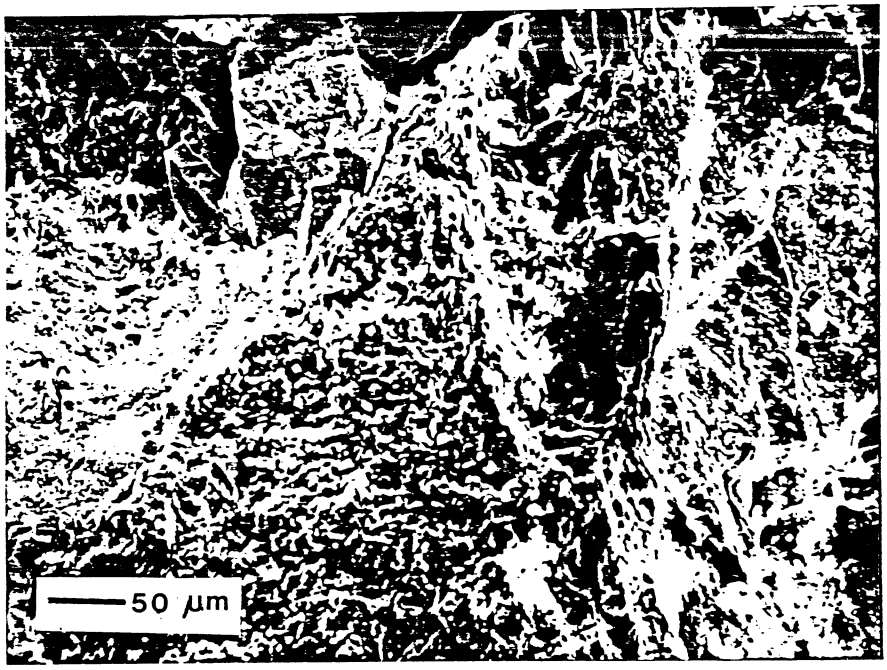

Figure 6. Cracking within the sericite region of Figure 4.

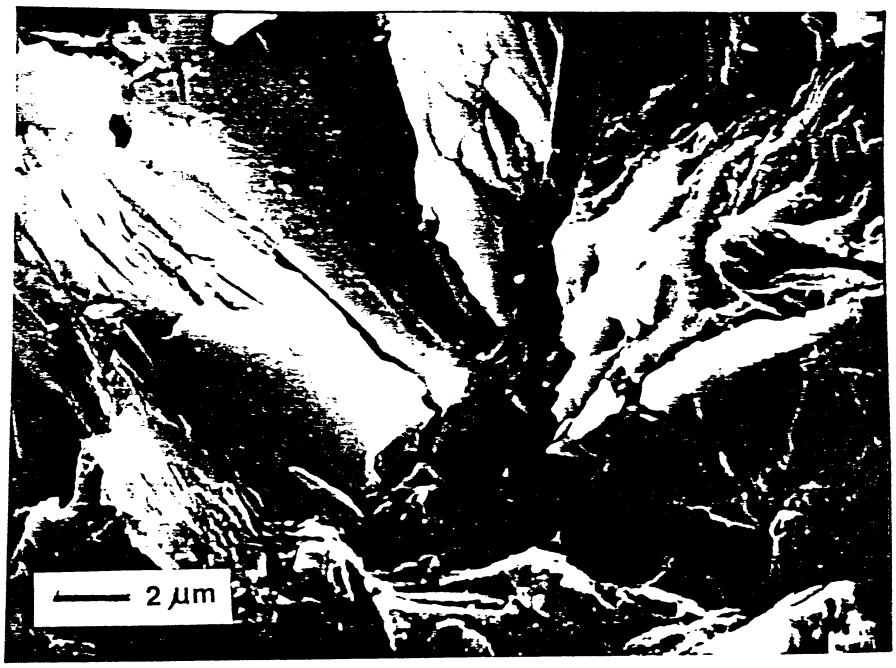

Figure 7. Intragranular and boundary cracks shown in sericite of Figure 6.

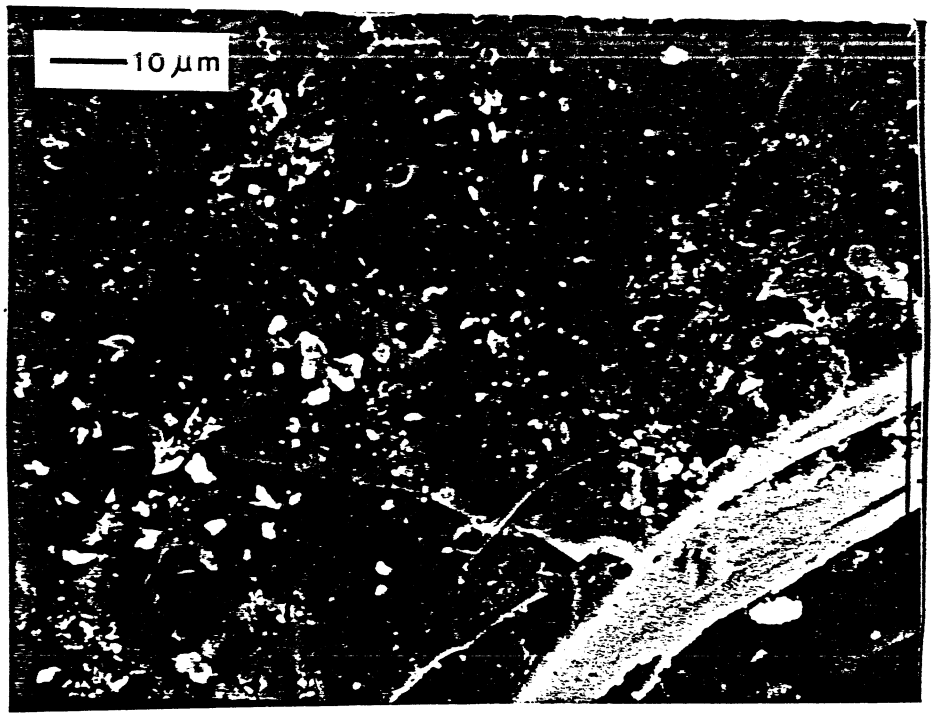

Figure 8. Transgranular cracks prevelent in quartz taken from specimen center for specimen 8.0-1.

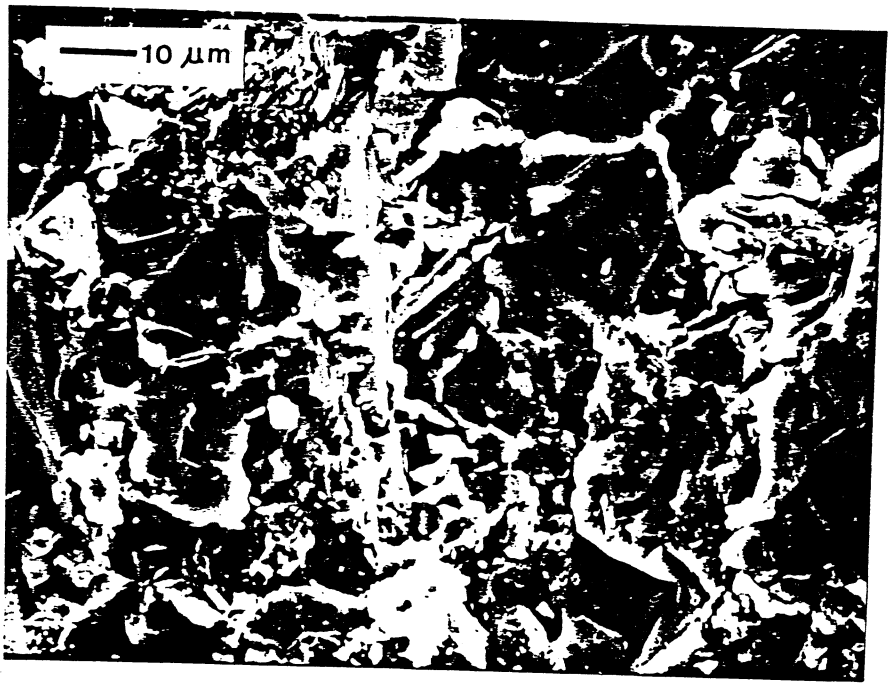

Figure 9. Numerous grain boundary cracks shown in specimen 8.0-1 in orthoclase.

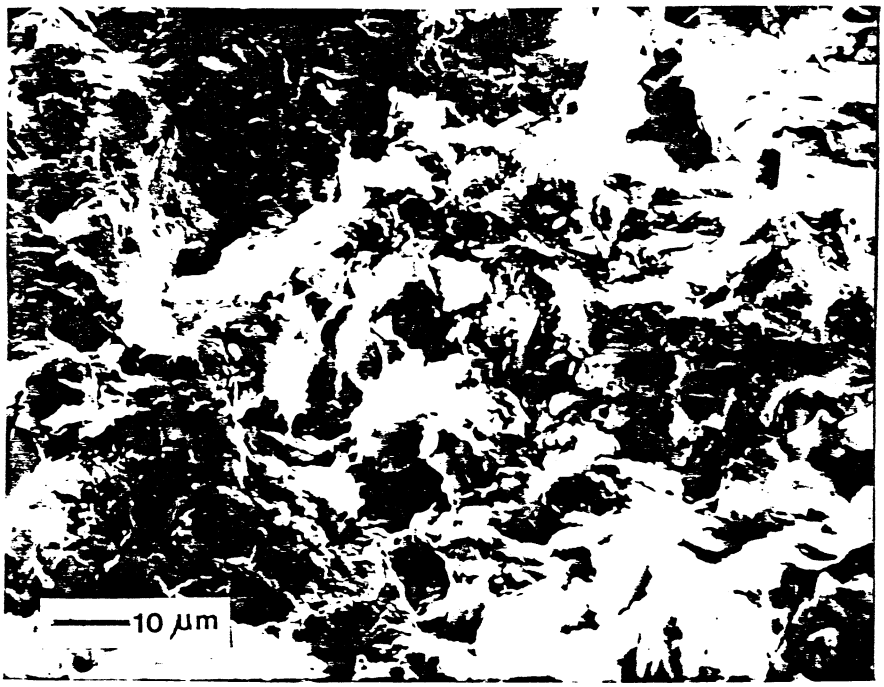

Figure 10. Unshocked specimen of sericite showing natural void structure.

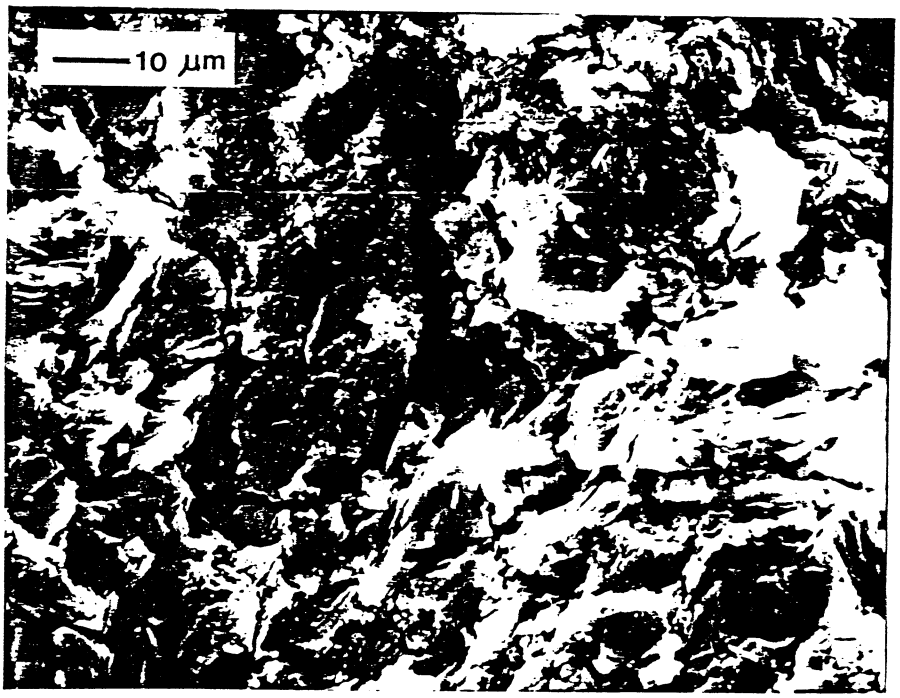

Figure 11. Shocked specimen 8.0-1 showing abundant cracking in sericite.

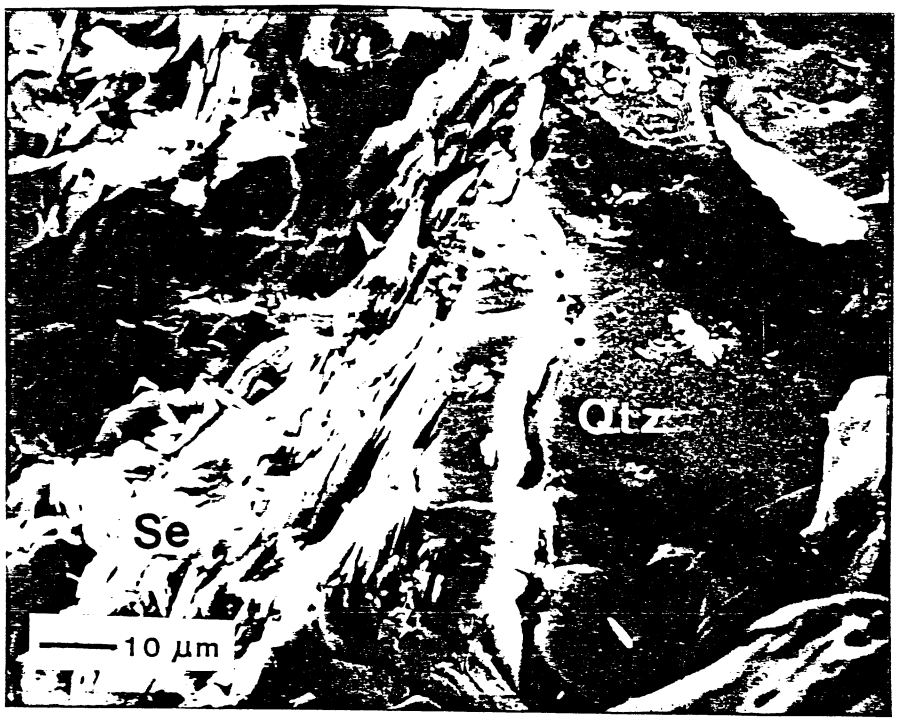

Figure 12. Grain boundary crack apparent between quartz (Qtz) and sericite (Se) in specimen 3.2-2; note internal microflaws as intragranular cracks isolated in the quartz.